PHYSICAL REVIEW B **71**, 180502(R) (2005)

Magnetically induced splitting of a giant vortex state in a mesoscopic superconducting disk

D. S. Golubović,[1] M. V. Milošević,[2] F. M. Peeters,[2] and V. V. Moshchalkov[1]
[1]*Nanoscale Superconductivity and Magnetism Group, Laboratory for Solid State Physics and Magnetism, K. U. Leuven, Celestijnenlaan 200 D, B-3001 Leuven, Belgium*
[2]*Departement Fysica, Universiteit Antwerpen (Campus Middelheim), Groenenborgerlaan 171, B-2020 Antwerpen, Belgium*
(Received 24 December 2004; revised manuscript received 4 April 2005; published 11 May 2005)

The nucleation of superconductivity in a superconducting disk with a Co/Pt magnetic triangle was studied. We demonstrate that when the applied magnetic field is parallel to the magnetization of the triangle, the giant vortex state of vorticity three splits into three individual Φ_0 vortices, due to a pronounced influence of the C_3 symmetry of the magnetic triangle. As a result of a strong pinning of the three vortices by the triangle, their configuration remains stable in a broad range of applied magnetic fields. For sufficiently high fields, Φ_0 vortices merge and the nucleation occurs through the giant vortex state. The theoretical analysis of this reentrant behavior at the phase boundary, obtained within the Ginzburg-Landau formalism, is in excellent agreement with the experimental data.

DOI: 10.1103/PhysRevB.71.180502 PACS number(s): 74.78.Na, 75.75.+a, 74.25.Dw

The nucleation of superconductivity in mesoscopic samples, whose dimensions are comparable to the superconducting coherence length $\xi(T)$ and the penetration depth $\lambda(T)$, is substantially affected by the sample boundary (see Ref. 1 and references therein). It is well established that in circular mesoscopic disks and loops the onset of superconductivity mostly occurs through the giant vortex state (GVS) due to their cylindrical symmetry.[2] On the other hand, in superconducting squares and triangles for certain magnetic fields the GVS easily splits into individual Φ_0 vortices (Φ_0 is the superconducting flux quantum), with a possible generation of additional antivortices.[3] The transition from the GVS to a set of Φ_0 vortices is caused by the reduced axial symmetry of squares and triangles and ensures that a vortex pattern conforms to the symmetry imposed by the boundary of the sample.

In this paper we investigate the onset of superconductivity in a mesoscopic disk on which a magnetic triangle with out-of-plane magnetization is placed. The nucleation of superconductivity in hybrid superconductor-ferromagnet disks and loops has been studied previously, both experimentally and theoretically, as these are a good model system to gain insight into the interplay between superconductivity and magnetism.[5–8] In this paper we show that the *symmetry* of the magnetic triangle has a profound effect on the onset of superconductivity in the disk. Due to the competition between the cylindrical symmetry of the superconducting disk and the C_3 symmetry of the stray field, superconductivity nucleates as a GVS for vorticity $L=2$, whereas for $L=3$ the GVS splits into three Φ_0 vortices. As a result of a strong pinning of the three individual vortices their configuration remains stable for $L=4$ and $L=5$.

The sample was prepared by electron beam lithography, using a double resist technique and lift-off in two steps. For details we refer to Ref. 6. In the first step, 30-nm Al disks were prepared using thermal evaporation. Upon the alignment, in the second step, Co/Pt magnetic triangles with the designed size of 650 nm were grown by electron beam evaporation on the disks. Some disks were left without magnetic elements to be used as reference samples. The Co/Pt magnetic triangle consists of a 2.5-nm Pt buffer layer and 10 bilayers of Co and Pt with thicknesses of 0.4 and 1 nm, respectively. The triangle is separated from the superconducting disk by a 2-nm Si spacer layer to avoid the proximity effect and suppression of the order parameter in the disk below the magnetic triangle. Co/Pt multilayers are known to have a pronounced perpendicular (out-of-plane) anisotropy.[9] The coercive field of the coevaporated reference film is 170 mT at room temperature, with a 90% remanence. The calculated spatial profile of the stray field $B_z(x,y)$ generated by the triangle is shown in Fig. 1(a), whereas Fig. 1(b) shows a magnetic force microscopy image (MFM) of the triangle taken at room temperature with no applied magnetic field, upon saturating it in the perpendicular magnetic field of 800 mT. The magnetic force microscopy image confirms that the triangle is in the single domain state. The brighter contrast along the edges corresponds to a higher stray field. It has been assumed that, upon the saturation, applied magnetic fields in the range ±15 mT did not affect the magnetization of the triangle during the measurements.

A scanning electron micrograph of the structure is shown

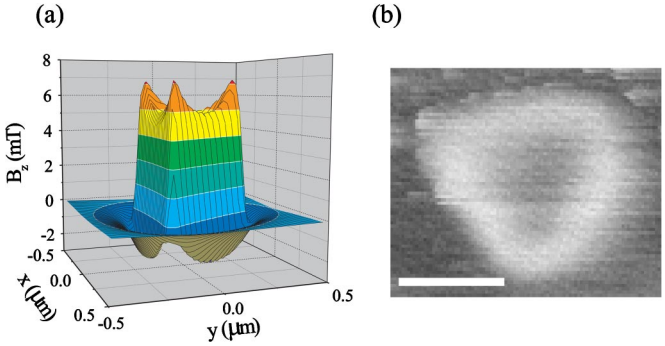

FIG. 1. (Color online) The calculated spatial profile (a) of the stray field and (b) a magnetic force micrograph of the triangle. The field values were calculated using the saturation magnetization of bulk Co. The white bar in (b) corresponds to 0.5 μm.

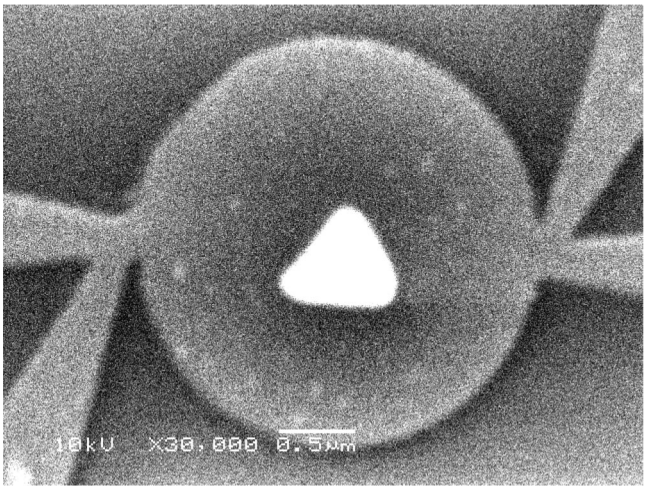

FIG. 2. A scanning electron micrograph of the structure.

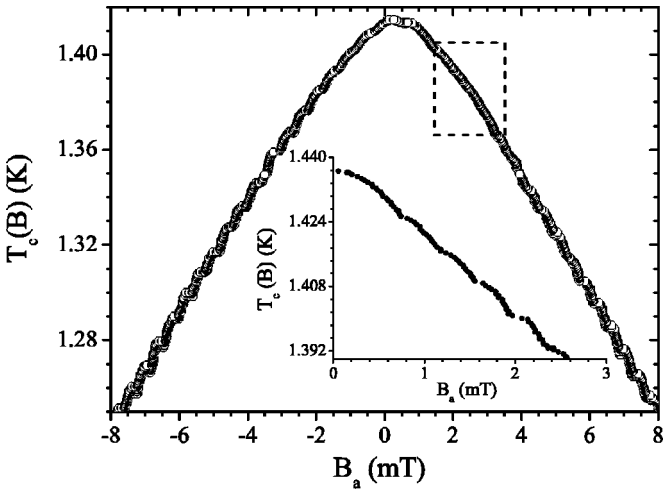

FIG. 3. Experimental $T_c(B)$ phase boundary of a superconducting disk with a magnetic triangle on top. The dashed square indicates the temperature region where no cusps in the phase boundary are observed. The inset shows a part of the $T_c(B)$ phase boundary of a reference disk down to 1.39 K.

in Fig. 2. The radius of the disk is 1.34 μm, which exceeds approximately 3% the patterned radius, whereas the sides of the triangle are 690, 650, and 740 nm, due to a relatively low acceleration voltage and a lack of the proximity correction tool in our e-beam system.

The superconducting $T_c(B)$ phase boundary was obtained by four-point transport measurements in a ^{4}He cryogenic setup at temperatures down to 1.25 K with the temperature stability of 0.4 mK, applying the magnetic field perpendicularly to the sample surface. A transport current with the effective value of 100 nA and frequency 27.7 Hz was used. The measurements were taken by sweeping the magnetic field at a constant temperature. The temperature and field steps were 0.5 mK and 50 μT, respectively. A special attention was being paid to eliminate any possible trapped flux in the setup during the measurements. The room temperature resistance and the residual resistance at 4.2 K of the structure shown in Fig. 2 are 6.5 and 3.2 Ω, respectively. The mean free path of Al, estimated from the coevaporated reference film, is 12.3 nm, so that the samples are in the dirty limit with the coherence length $\xi(0)=120$ nm. The critical temperature of the disk with the triangle in zero applied field is $T_{c0}=1.4136$ K, whereas for the reference disk is $T_{c0}^{(R)}=1.4366$ K.

Hereafter we will be referring to a magnetic field applied parallel to the magnetization of the triangle as positive.

The experimental superconducting $T_c(B)$ phase boundary is shown is Fig. 3. The inset is a part of the $T_c(B)$ phase boundary of a reference superconducting disk, without the magnetic triangle, down to $0.967T_{c0}^{(R)}$. The shift of the $T_c(B)$ phase boundary along the field axis, with the maximum critical temperature T_{cm} attained for a finite value of an applied magnetic field, was already previously observed and is caused by the compensation of the stray field generated by the dot.[6,7] It can be seen that for negative applied fields the $T_c(B)$ phase boundary exhibits a typical cusplike behavior in the whole temperature range, with each cusp corresponding to a change in vorticity by one. However, for positive applied fields there are no cusps in the $T_c(B)$ phase boundary for a broad range of temperatures between $0.991T_{cm}$ and $0.969T_{cm}$. The region is indicated by a dashed square in Fig. 3. For lower temperatures, the cusplike behavior is recovered. In the same relative temperature range, the $T_c(B)$ phase boundary of a reference superconducting disk exhibits the typical behavior.[4]

The experimental data were analyzed in the framework of the Ginzburg-Landau (GL) theory. The three-dimensional GL equations were solved numerically, without imposing any constraints on the final form of the order parameter at a given temperature and magnetic field (for details of the approach, see Ref. 10 and references therein). At the superconductor-vacuum interface, the Neumann boundary condition for the order parameter was used. The influence of the current and voltage contacts on the nucleation process was modeled by adding two stripes with a length of 400 nm and a width of 250 nm to the disk, at the position of the current contacts. Even though they geometrically differ from the real contacts, they allow for a slight local spread of the screening currents in the disk, as well as provide a local enhancement of the superconductivity in the contact area. Therefore, they may be used to adequately describe the physical phenomena related to the real contacts. The simulations were carried out with the exact dimensions of the disk and triangle, using the saturation magnetization of bulk Co $M=140$ mT, with the coherence length as a fitting parameter. The experimental results were theoretically best reproduced with $\xi(0)=118$ nm, which is in excellent agreement with the coherence length obtained for the reference film.

Figure 4 shows the experimental and theoretical $T_c(B)$ phase boundaries of the disk with the triangle, down to $0.95T_{cm}$. Open symbols are the experimental data, whereas the solid line presents the theoretically obtained phase boundary. The numbers indicate vorticities and arrows point the field values at which a particular transition occurs. The inset shows the $dT_c(B)/dB_a$ versus the applied field B_a. The stray field of the triangle creates one vortex in the disk in the absence of the external magnetic field. The state without vor-

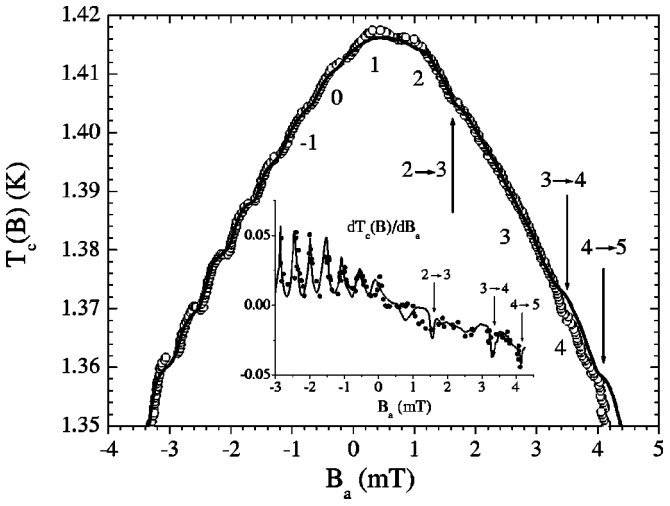

FIG. 4. $T_c(B)$ phase boundary of a superconducting disk with a magnetic triangle. The solid line presents the theoretical curve, whereas open symbols show experimental data. The numbers stand for the vorticity, with arrows indicating the transitions between the states with different vorticities. The inset shows the $dT_c(B)/dB_a$ vs the applied field. The filled symbols are experimental data and line is the theoretical curve.

tices ($L=0$) is, therefore, realized by applying small negative magnetic fields. For negative applied fields, the nucleation of superconductivity occurs through the GVS, which is reflected by a regular cusplike character of the $T_c(B)$ phase boundary. The contour plot of the phase of the order parameter for $L=-3$, shown in Fig. 5, illustrates the presence of the GVS.

The GVS is retained in positive applied fields for up to $L=2$. However, for vorticity $L=3$ the lowest energy state corresponds to three Φ_0 vortices. The contour plots of the phase of the order parameter for the $L=2$ and $L=3$ are shown in Fig. 5. It is clear that the state $L=2$ is a GVS located below the triangle, whereas for $L=3$ there are three individual vortices, located towards the apices of the triangle. The three Φ_0 vortices are strongly pinned at their positions by the triangle. This results in a substantially enhanced stability of the $L=3$ state, and gives rise to an extended cusp in the $T_c(B)$ phase boundary. The configuration of the three cornered vortices is imposed by the symmetry and remains stable for $L=4$ and $L=5$. For higher applied fields (and consequently higher vorticities), vortices are compressed under the triangle at the center of the disk and forced by the screening currents to merge back to the GVS. This reentrantlike behavior is reflected by the reappearance of regular cusps in the $T_c(B)$ phase boundary for higher fields (see Fig. 3).

In addition to the character and symmetry of the boundary, the onset of superconductivity in hybrid superconductor-ferromagnet structures is profoundly influenced by the stray field locally generated by the magnetic element. The extent of the influence depends on the mutual relation between the parameters of the superconductor and the ferromagnet. As detailed in Ref. 11, with perpendicularly magnetized dots the lowest energy state is achieved when an external vortex is located below the dot (in the parallel case), whereas an eventual antivortex is repelled and its equilibrium position is de-

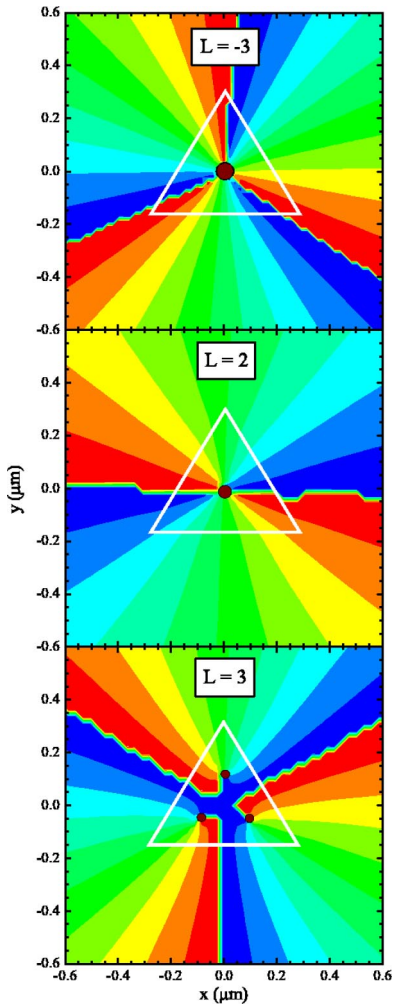

FIG. 5. (Color online) The contour plot of the phase of the order parameter for the vorticities $L=-3$, $L=2$, and $L=3$. The blue-red colors are $0/2\pi$ of the phase. The white triangle illustrates the position of the magnetic triangle.

termined by other relevant parameters. As a general rule, the prevailing mechanism that governs the vortex behavior is its interaction with the screening currents generated by the stray field of a magnetic dot.

For negative applied fields, which generate antivortices with respect to the direction of the magnetization of the triangle, the symmetry of the triangle does not have a major influence on the nucleation process, because the triangle and external field induce opposite supercurrents in the disk, which tend to cancel each other. With increasing negative applied field, the vortexlike currents prevail and after the critical conditions are reached antivortices nucleate. The onset occurs through the GVS, as imposed by the cylindrical symmetry of the disk. For positive applied fields, on the other hand, there exists a competition between the cylindrical symmetry of the superconducting disk and the C_3 symmetry of the magnetic triangle, which governs the onset. Both currents, induced by the externally applied field and by the triangle, compress the vortices to the center of the disk, but imposing different geometries on the final vortex configuration. For $L=1$ and $L=2$, the distribution of the order param-

eter is influenced by the symmetry of the magnetic triangle through the suppression of the order parameter under its edge,[11] but there is no particular correspondence between the vortex patterns and the symmetry of the stray field. For $L=3$, however, the C_3 symmetry of the triangle has a pronounced influence and the GVS splits into three Φ_0 vortices. This splitting is caused by the tendency of the system to minimize its kinetic energy, associated with the screening currents. This process can be thought of as the competition between the triangularly imposed confinement, compressing vortices to its center and their mutual repulsion. Therefore, due to the C_3 symmetry, only the state $L=3$ may actually be stabilized as a collection of Φ_0 vortices. The vortices assume the positions close to the apices of the triangle, where the positive stray field is the highest.

Given that the specific distribution of the screening currents following from the shape of the triangle, the configuration of the three Φ_0 vortices that minimizes the kinetic energy remains favorable and stable in a broad range of applied fields, that is, the three vortices are strongly pinned at their positions. The enhanced temperature stability range follows from the size constraints of the pinning site. Namely, the fourth vortex can only enter under the triangle when the pinning area becomes large enough in terms of $\xi(T)$, so that the pinning force overwhelms the vortex repulsion. The fourth vortex is then pushed to the center of the triangle, without causing any substantial rearrangement of the three vortices. For vorticity $L=5$ three Φ_0 vortices remain stable and pinned at the apices of the triangle, whereas a GVS with a vorticity 2 is created at the center of the triangle. For higher fields, the vortices below the triangle merge, forming a single GVS state. We report on the observation of such a reentrant behavior at the phase boundary.

In conclusion, we have investigated the onset of superconductivity in a mesoscopic superconducting disk with a perpendicularly magnetized magnetic triangle and demonstrated that the symmetry of the magnetic triangle strongly affects the nucleation process. For negative applied fields, the onset of superconductivity is predominantly influenced by the boundary of the disk and occurs through the GVS, whereas for positive applied fields the GVS with vorticity $L=3$ splits into three Φ_0 vortices. This magnetically induced splitting of the GVS at the phase boundary is generally applicable to mesoscopic superconductors with magnetic polygons on top, where the number of apices would determine the particular vorticity at which the GVS splits into a set of Φ_0 vortices. Therefore, these structures can be employed as a tool to manipulate vortex configurations and achieve an enhanced stability of a particular vortex state, using a simple physical mechanism.

This work was supported by the Research Fund K. U. Leuven GOA/2004/02 program, the University of Antwerp (GOA), the Flemish FWO and the Belgian IUAP programs, as well as by the JSPS/ESF "Nanoscience and Engineering in Superconductivity" program.

[1] V. V. Moshchalkov *et al.*, Nature (London) **373**, 319 (1995).

[2] V. A. Schweigert, F. M. Peeters, and P. S. Deo, Phys. Rev. Lett. **81**, 2783 (1998); A. K. Geim *et al.*, Nature (London) **390**, 259 (1997); V. Bruyndoncx *et al.*, Phys. Rev. B **60**, 10 468 (1999); A. Kanda *et al.*, Phys. Rev. Lett. **93**, 257002 (2004).

[3] L. F. Chibotaru *et al.*, Nature (London) **408**, 833 (2000); Phys. Rev. Lett. **86**, 1323 (2001); V. R. Misko *et al.*, *ibid.* **90**, 147003 (2003).

[4] B. J. Baelus, F. M. Peeters, and V. A. Schweigert, Phys. Rev. B **63**, 144517 (2001); W. V. Pogosov, *ibid.* **65**, 224511 (2002).

[5] M. V. Milošević, S. V. Yampolskii, and F. M. Peeters, Phys. Rev. B **66**, 024515 (2002).

[6] D. S. Golubović *et al.*, Phys. Rev. B **68**, 172503 (2003).

[7] D. S. Golubović *et al.*, Europhys. Lett. **65**, 546 (2004).

[8] A. Y. Aladyshkin, A. S. Mel'nikov, and D. A. Ryzhov, J. Phys.: Condens. Matter **38**, 6591 (2003); J. E. Villegas *et al.*, Science **302**, 1188 (2003); M. Lange *et al.*, Phys. Rev. Lett. **90**, 197006 (2003).

[9] P. F. Carcia, J. Appl. Phys. **63**, 10 (1998); J. V. Harzer *et al.*, *ibid.* **69**, 2448 (1991).

[10] V. A. Schweigert and F. M. Peeters, Phys. Rev. B **57**, 13 817 (1998).

[11] M. V. Milošević and F. M. Peeters, Phys. Rev. B **68**, 094510 (2003); **69**, 104522 (2004).